

Experimental Studies

Biochemical Inhibition of DOG1/TMEM16A Achieves Antitumoral Effects in Human Gastrointestinal Stromal Tumor Cells *In Vitro*

ROBIN FRÖBOM¹, FELIX SELLBERG², CHENG XU³, ALLAN ZHAO³, CATHARINA LARSSON^{4,5},
WENN-ONN LUI^{4,5}, INGA-LENA NILSSON¹, ERIK BERGLUND⁶ and ROBERT BRÄNSTRÖM¹

¹Department of Molecular Medicine and Surgery, Karolinska Institutet, Stockholm, Sweden;

²Department of Immunology, Genetics and Pathology, Uppsala University, Uppsala, Sweden;

³The Rolf Luft Center for Diabetes Research, Department of Molecular Medicine and Surgery, Karolinska Institutet, Stockholm, Sweden;

⁴Department of Oncology-Pathology, Karolinska Institutet, Stockholm, Sweden;

⁵Cancer Center Karolinska, Karolinska University Hospital, Stockholm, Sweden;

⁶Division of Transplantation Surgery, CLINTEC, Karolinska Institute, and Department of Transplantation Surgery, Karolinska University Hospital, Stockholm, Sweden

Abstract. *Background/Aim:* DOG1 is a calcium-activated chloride channel that has gained attention as a promising drug target due to its involvement in several processes essential for tumor development and progression. DOG1 is overexpressed in >95% of gastrointestinal stromal tumors (GIST). The aim was to determine DOG1 inhibition antitumoral effects on GIST. *Materials and Methods:* Human GIST (GIST-T1 and GIST882) cell lines were used to study the effect of DOG1 inhibitors on chloride currents, viability, colony formation, and cell cycle. *Results:* CaCC_{inh}-A01 decreased chloride currents. CaCC_{inh}-A01 and T16_{inh}-A01 reduced GIST cell viability and CaCC_{inh}-A01 affected cell cycle distribution leading to G₁ cell-cycle arrest. CaCC_{inh}-A01 also increased the sub-G₁ phase population, indicative of apoptosis, in GIST882. CaCC_{inh}-A01 strongly reduced the colony forming ability of the cells, whereas T16_{inh}-A01 did not. *Conclusion:* DOG1 inhibition has antitumoral effects in GIST cells in vitro, and could potentially serve as a target for GIST therapy.

Gastrointestinal stromal tumor (GIST) is of mesenchymal origin and is the most common soft tissue sarcoma (1). In

most cases, it is characterized by *gain-of-function* mutations in genes coding for receptor tyrosine kinases (e.g. KIT and PDGFRA) (2). Current medical treatment is targeting this mutated receptor with tyrosine kinase inhibitors, and this has greatly improved the survival in GIST (3). Discovered-on-GIST-1 (DOG1) and synonymous with TMEM16A and ANO1, belongs to the group of calcium-activated chloride channels (CaCCs) and has proven to be an important diagnostic marker due to its expression in >95% of GISTs (4). The gene, *ANO1*, coding for the DOG1 protein is located in a commonly amplified region of the long arm of chromosome 11 (11q13.3) in human cancers (5). DOG1 has not been found to be mutated in GIST (6), however, DOG1 is expressed in interstitial cells of Cajal (7), which is the proposed progenitor cell of GIST (2).

CaCCs are expressed in a variety of tissues and are essential regulators of normal physiological functions, including neuronal excitability, smooth muscle cell contraction, epithelial fluid secretion, and gastrointestinal motility (8). Specifically, DOG1 has been shown to be a voltage-sensitive and ligand-activated ion channel that is activated by increased intracellular free Ca²⁺ ([Ca²⁺]_i) (9). Increasing evidence suggests that DOG1 is involved in tumorigenesis, cancer progression, metastasis, and cell survival. It has been studied in several tumors of epithelial origin such as: i) breast (10-13), ii) lung (14), iii) colon (15, 16), iv) head and neck (17-19), v) gastric (20), vi) glioma (21), and vii) prostate (22, 23). The reported effects have been conflicting, and several mechanisms have been proposed. Signaling pathways of relevance are EGFR and CAMKII (13, 24), MAPK (17), TGF-β (25), and NF-κB (21), which seem to be cell-specific. A recent study showed that the apoptosis signaling pathway

This article is freely accessible online.

Correspondence to: Robin Fröbom, Endocrine and Sarcoma Surgery Unit, Department of Molecular Medicine and Surgery, Karolinska Institutet, Karolinska University Hospital L1:03, SE-171 76 Stockholm, Sweden, E-mail: robin.frobom@ki.se

Key Words: Gastrointestinal stromal tumors, GIST, DOG1, TMEM16A, ion channel, cancer.

activated through TNF- α was similar between the knockdown model and a biochemical inhibition (23). In GIST, high DOG1 expression is associated with poor prognosis and its high levels in circulating tumor cells can predict recurrence (26). The functional role of DOG1 is not fully understood, with only two studies having examined its role in GIST to date. The first used either DOG1 knockdown or biochemical inhibition. Using the knockdown approach resulted in decreased growth rate in the GIST xenografts *in vivo*, while no effect on cell growth was seen *in vitro* by either DOG1 knockdown or biochemical inhibition (27). The second study by our group used activator and inhibitor (T16_{inh}-A01) of DOG1 channel and studied several cell biological properties in an *in vitro* setting, and determined that DOG1 inhibition induces apoptosis in an imatinib-resistant cell line (28). In a study using several epithelial tumor cell lines, it was discovered that DOG1 degradation was crucial for its antitumoral effects (29). Since then, advancements have been made in the knowledge of CaCC inhibitors possessing not only inhibitory activities but also DOG1 protein degradation properties, reviewed in detail elsewhere (30). Therefore, we sought to evaluate if enhanced DOG1 inhibition would lead to functional antitumoral effects in well-established GIST tumor cell lines.

Materials and Methods

Cell lines. GIST-T1 (Cosmo Bio Co. Ltd., Tokyo, Japan) and GIST882 are two human GIST cell lines. GIST-T1 were maintained in Dulbecco's Modified Eagle Medium (DMEM) supplemented with 10% fetal bovine serum (FBS), 1% Glu-Max, 1% Penicillin-Streptomycin. GIST882 cells were maintained in DMEM, 15% FBS, 1% Glu-Max, 1% Penicillin-Streptomycin. Cells were incubated in 37°C with 5% CO₂. Reagents for medium were purchased from Sigma-Aldrich (Sigma-Aldrich, MO, USA). Both cell lines have been shown to express DOG1 (27). GIST882 cell line was a kind gift from professor Jonathan A. Fletcher, Brigham Women's Hospital (MA, USA).

Reagents. Two inhibitors were used to modulate channel activity. T16_{inh}-A01 (Sigma-Aldrich) has previously been shown to reduce chloride currents by up to 60% at a concentration of 30 μ M in GIST cells (28). CaCC_{inh}-A01 (Sigma-Aldrich) has been shown to reduce chloride currents in DOG1 expressing cells (29). E-act (Sigma-Aldrich) was used to activate the chloride channel in patch-clamp experiments only. Stock solutions were dissolved in dimethyl sulfoxide (DMSO) yielding stock solutions of 10 mM. Solvent (DMSO) was used as a control, and concentrations never reached >0.3% (vol/vol).

Electrophysiology. Whole-cell CaCC currents were recorded using the patch-clamp technique (31) and a HEKA EPC-10 patch-clamp amplifier (HEKA Elektronik, Germany). Current traces were shown according to the convention that up-ward deflection denotes inward currents, using extracellular solution (*i.e.* bath solution) contained: i) 150 mM NaCl, ii) 1 mM MgCl₂, iii) 1 mM CaCl₂, iv) 10 mM Glucose, v) 10 mM Mannitol and vi) 10 mM Na-HEPES (pH 7.4). The pipette (*i.e.* intracellular) solution contained: i) 130 mM CsCl, ii) 1 mM MgCl₂, iii) 10 mM HEPES, and iv) 1 mM ATP (pH 7.4 using CsOH).

CaCl₂ and EGTA were added to the pipette solution to obtain the desired free Ca²⁺-concentration, [Ca²⁺]_{pip}: i) 8 mM CaCl₂ and 10 mM EGTA for 305 nM, and ii) 8 mM CaCl₂ and 12 mM EGTA for 90 nM (calculated with MaxChelator software version 1.3 developed by Dr. Chris Patton, Stanford University, USA, <http://maxchelator.stanford.edu>). In all whole-cell recordings, series resistance (R_s) was <40 M Ω , and cell capacitance was updated between every voltage-protocol cycle. All experiments were performed at room temperature, approximately +22°C, and cells were voltage-clamped at -80 mV and subsequently depolarized for 600 ms in +20 mV steps until +80 mV. Pipettes were pulled from borosilicate using a P-2000 laser pipette puller (Sutter Instruments, Novato, CA, USA) and had resistances between 2 and 4 M Ω . Records were filtered at 2.1 kHz and digitized at 10 kHz. Mean whole-cell current was calculated for each voltage-step between 100 ms after voltage-pulse started, and 100 ms prior to voltage-pulse ended.

Cell viability assay. Cells were seeded in 96-well plates at a concentration of 0.5×10⁴ cells per well followed by incubation overnight to allow adherence. Twenty-four hours later cells were treated with each compound respectively or DMSO as a control, at these time points: i) 24 h, ii) 48 h, and iii) 72 h. CellTiter-Glo (Promega, WI, USA), an ATP-based luminometric method, was used to determine cell viability, according to manufacturer's protocol. In short, cells were taken out from incubator, 100 μ L of CellTiter-Glo reagent at room temperature were added into each well, and the plate was put on a shaker for 15-minutes and was left to stabilize for 5-10 minutes before the readout. For subsequent analysis, all values were normalized to control. Readout was done using GloMax 96 Microplate Luminometer (Promega).

Cell cycle analysis. Cells were seeded at a density of 1×10⁵ in 6-well plates and were left to adhere overnight. Drugs, or DMSO, were added to each well and were incubated for 48 hours. Following treatment, adherent cells were washed with PBS twice, were harvested and subsequently fixed in 70% cold ethanol. Cells were fixed at 4°C for at least 2 h, they were then washed and incubated for 30 minutes in propidium iodide (PI) staining buffer (10 μ g/ml PI and RNase A 100 μ g/ml, Sigma-Aldrich) at room temperature. Cytometry was performed using a FACSVerse flow cytometer (BD Biosciences, San Jose, CA, USA). Data were analyzed using Flow Jo software and cell cycle analysis was done using a built-in tool with Watson (pragmatic) univariate model. Experiments were performed in triplicates.

Colony Formation assay. GIST-T1 cells were seeded in 12-well plates with approximately 1,000 cells/well. Cells were incubated overnight to allow adhering, after which cells were treated with the DOG1 inhibitory compounds. No media change occurred during the 10-14 days of the experiment. After 10-14 days, cells were fixed and stained using a solution of 4% phosphate-buffered formaldehyde with 0.5% crystal violet (wt/vol). Well plates were scanned using LI-COR Odyssey CLx scanner with subsequent quantification of each well in Image Studio LI-COR software (both from LI-COR Biosciences, NE, USA).

Statistical analysis. All data are presented as mean±standard error of the mean (SEM) unless otherwise stated. Experiments were done in at least triplicates unless otherwise stated. For electrophysiology, *t*-test was used. For the viability assay, two-way

ANOVA was used with Tukey's test for multiple comparisons. For the cell cycle analysis, two-way ANOVA and *post-hoc* analysis using Dunnett's test were implemented. For the sub- G_1 analysis, Kruskal-Wallis test was used with Dunn's test for multiple comparisons. For the colony formation assay, one-way ANOVA with Dunnett's test for multiple comparisons was used. A *p*-Value of less than 0.05 was considered to be statistically significant. All analyses were performed using GraphPad Prism software 7.0 (GraphPad Software Inc., SD, CA, USA).

Results

The inhibitor CaCC_{inh}-A01 reduces chloride currents in GIST cells. To assess chloride currents, we used the patch-clamp technique in single cells (Figure 1). Exposure of the compound CaCC_{inh}-A01 (30 μ M) resulted in decreased currents of approximately 50% (Figure 1A and B). At +80 mV, the mean current decreased from 399.1 ± 35 to 164.4 ± 8 pA ($p < 0.01$, $n = 4$). CaCC_{inh}-A01 showed a dose-dependent inhibition of chloride currents, and $69.8 \pm 45.2\%$ ($n = 3$) activation by DOG1-activator (E-act) (Figure 1C). Following washout, chloride currents increased (Figure 1E). Significant difference was observed following exposure of 30 μ M CaCC_{inh}-A01. In experiments where pipette solutions contained 90 nM of $[Ca^{2+}]_{pip}$, low chloride currents could be observed, but none were activated by E-act 30 μ M (Figure 1D).

DOG1 inhibition leads to decreased cell viability in GIST cells. GIST cells were treated for 24, 48, or 72 h before measurement of cell viability expressed by the percentage of control. Both CaCC_{inh}-A01 and T16_{inh}-A01 treated cells showed decreased viability as compared to DMSO-control (Figure 2). At time point 72-h, both cell lines showed reduced viability at 30 μ M of CaCC_{inh}-A01 or T16_{inh}-A01. In GIST-T1 cells, CaCC_{inh}-A01 (30 μ M) reduced their viability to 70% compared to control ($p < 0.0001$), while T16_{inh}-A01 (30 μ M) reduced it to 64% compared to control ($p < 0.0001$). In GIST882 cells, 30 μ M of CaCC_{inh}-A01 reduced cell viability to 66% compared to control ($p < 0.0001$) and T16_{inh}-A01 reduced it to 88% ($p = 0.012$). Similar effects were observed between the two cell lines using CaCC_{inh}-A01, however, T16_{inh}-A01 was more potent in GIST-T1 (Figure 2E).

DOG1 inhibition decreases colony formation. To assess the long-term effects of DOG1 inhibition, a colony formation assay was used. GIST-T1 showed a distinct decreased colony formation ability following CaCC_{inh}-A01 treatment compared to T16_{inh}-A01 (Figure 1A). For CaCC_{inh}-A01 treated cells, significantly reduced ability of GIST-T1 cells to form colonies was observed for concentrations over 3 μ M compared to control (Figure 3B), with 5 μ M ($p < 0.05$), 10 μ M ($p < 0.001$), and 30 μ M ($p < 0.0001$). In T16_{inh}-A01 treated cells, no significant difference was found (Figure 3C).

CaCC_{inh}-A01 treatment leads to G_1 -arrest in GIST cells. Adherent cells were used for cell cycle analysis after 48-hour treatment with CaCC_{inh}-A01 or T16_{inh}-A01 (Figure 4). In GIST-T1, CaCC_{inh}-A01 changed the cell cycle distribution of the populations significantly compared to both T16_{inh}-A01 treated cells and DMSO control. Cells treated with CaCC_{inh}-A01 were arrested in G_1 -phase, with a 6% increase of cells in G_1 -phase with 10 μ M ($p < 0.01$) and 10% increase of cells in G_1 -phase with 30 μ M ($p < 0.001$) compared to control. T16_{inh}-A01 showed no statistically significant difference in the distribution of the populations compared to control (Figure 4E). In GIST882, G_1 cell cycle arrest was also noted in CaCC_{inh}-A01, but not in T16_{inh}-A01 treated cells (Figure 4F), corresponding to an increase of 6% in G_1 -phase for both concentrations, respectively, compared to control. In GIST882 cells, a sub- G_1 population corresponding to apoptotic cells, was significantly increased in 30 μ M with 6-7% showing signs of apoptosis ($p < 0.05$, Figure 4D), whereas in 10 μ M and in the control no statistically significant changes were observed, and sub- G_1 population ranged between 2-3%. This sub- G_1 fraction (Figure 4B) of cells were excluded from the cell cycle analysis, to allow comparison between viable cells capable of undergoing mitosis, with 100% viable portion present only in G_0/G_1 , S, and G_2/M phases. No significant sub- G_1 population was observed in GIST-T1.

Discussion

GIST is the most common human sarcoma in the abdominal cavity, with an incidence of about 15 per million patients/year. Since the introduction of tyrosine kinase inhibitor treatment little more than 15 years ago, tumor-specific survival has improved dramatically (3). However, the majority of patients develop resistance over time, and additional treatment strategies are a prioritized field in the GIST research area.

DOG1 has, ever since its discovery in GIST, been a reliable diagnostic marker due to its strong expression in GIST, with more than 95% positive specimens, regardless of the receptor tyrosine kinase mutational status (4). Functionally DOG1 belongs to the group of CaCCs, which are essential in a range of physiological processes, including cell volume regulation, smooth muscle cell signaling and neuronal signaling (8). In tumors of epithelial origin, DOG1 has become increasingly studied due to its involvement in several pathophysiological processes that are crucial for tumor development and progression (32).

Since DOG1 is abundantly expressed in GIST, the hypotheses have been that it would work as a therapeutic target. Two studies have examined this question, both failing to show antitumoral effects of DOG1 modulation *in vitro*. The first study by Simon *et al.*, has examined its role both in a cell line and a xenograft model, using a knockdown

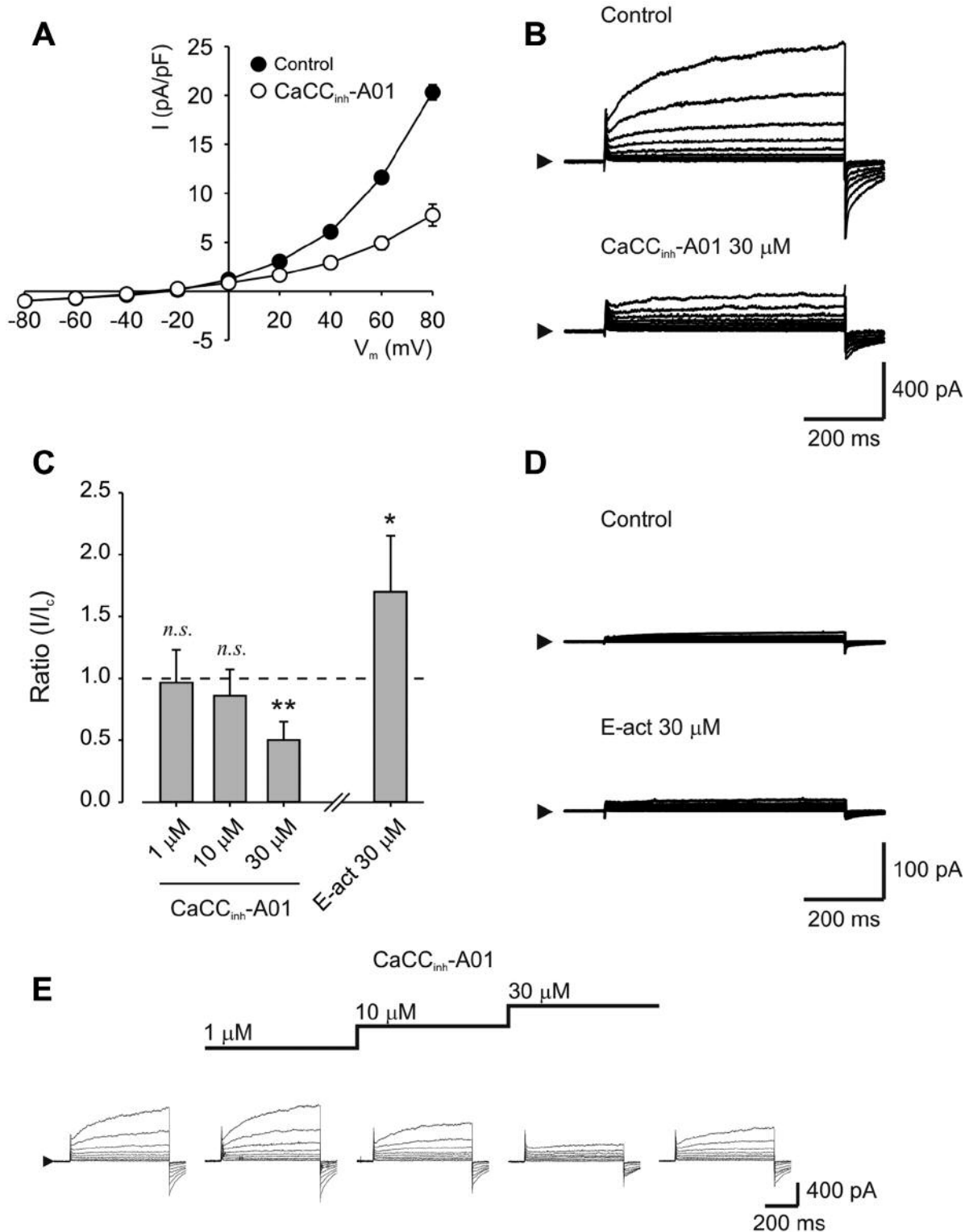


Figure 1. Patch-clamp recordings from GIST-T1 using whole-cell configuration. The cells were voltage-clamped at -80 mV and were subsequently depolarized for 600 ms in steps of 20 mV to $+80$ mV (A, B, and D). In A and B, $[\text{Ca}^{2+}]_{\text{pip}}$ was fixed to 305 nM, whereas in D $[\text{Ca}^{2+}]_{\text{pip}}$ was 90 nM. In C, the effect of the inhibitor $\text{CaCC}_{\text{inh}}\text{-A01}$ and the activator E-act was summarized in GIST-T1 cells. The effect of $\text{CaCC}_{\text{inh}}\text{-A01}$ was reversible since after withdrawal of the drug the whole-cell current returned the same level as before exposure to the drug (E). Arrowhead indicates zero current line in B, D, and E. Mean current was measured between 100 ms and 500 ms, and *denotes $p < 0.05$, ** $p < 0.01$. n.s.: Not significant.

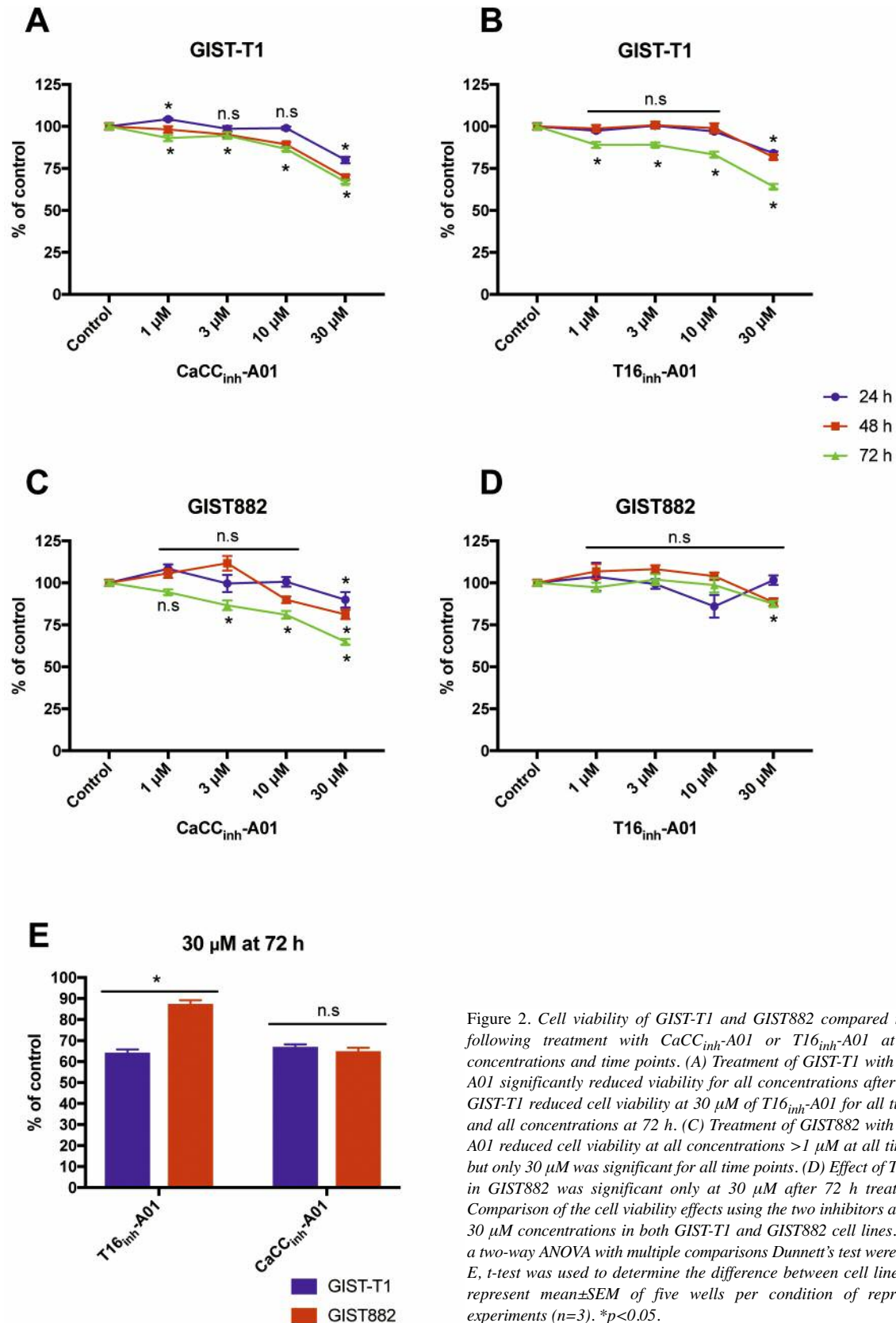


Figure 2. Cell viability of GIST-T1 and GIST882 compared to control following treatment with CaCC_{inh}-A01 or T16_{inh}-A01 at different concentrations and time points. (A) Treatment of GIST-T1 with CaCC_{inh}-A01 significantly reduced viability for all concentrations after 72 h. (B) GIST-T1 reduced cell viability at 30 μ M of T16_{inh}-A01 for all time points and all concentrations at 72 h. (C) Treatment of GIST882 with CaCC_{inh}-A01 reduced cell viability at all concentrations >1 μ M at all time points, but only 30 μ M was significant for all time points. (D) Effect of T16_{inh}-A01 in GIST882 was significant only at 30 μ M after 72 h treatment. (E) Comparison of the cell viability effects using the two inhibitors at 72 h and 30 μ M concentrations in both GIST-T1 and GIST882 cell lines. For A-D, a two-way ANOVA with multiple comparisons Dunnett's test were used. For E, t-test was used to determine the difference between cell lines. Results represent mean \pm SEM of five wells per condition of representative experiments (n=3). *p<0.05.

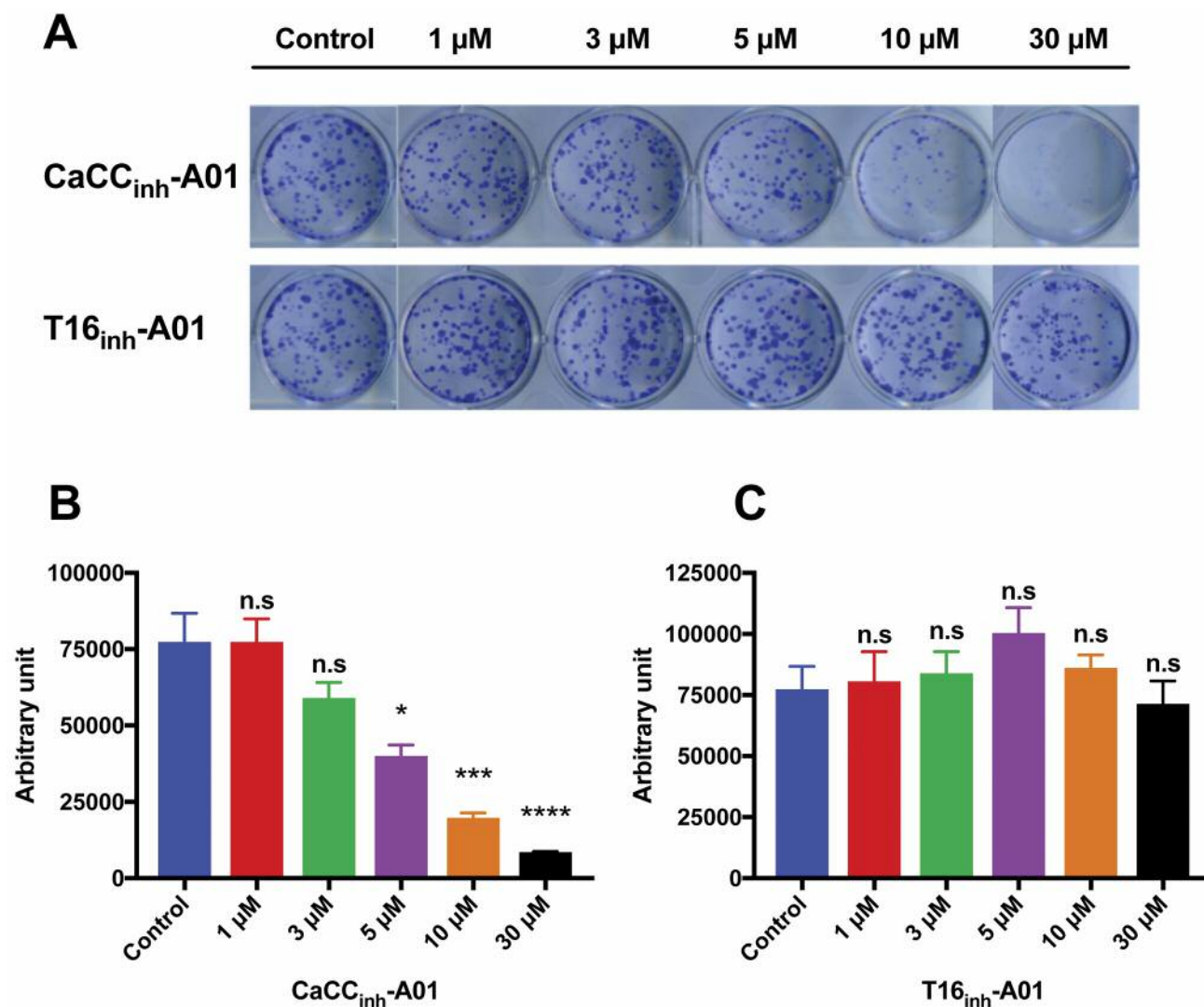


Figure 3. Colony formation assays in GIST-T1 cells. (A) Representative images of colony formation in GIST-T1 cells. Cells treated with various concentrations of CaCC_{inh}-A01 (upper row) or T16_{inh}-A01 (lower row) decreased colony-forming ability. (B) Quantitative values of colony forming ability in CaCC_{inh}-A01-treated cells, with a significantly reduced colony formation at concentrations $>3 \mu$ M. (C) Quantitative values of T16_{inh}-A01 treated cells, with no significant change in colony formation. Results represent mean \pm SEM (n=3). Analysis of variance was done using one-way ANOVA with multiple comparison tests using Dunnett's test. * $p < 0.05$, *** $p < 0.001$, **** $p < 0.0001$.

approach as well as biochemical inhibition (27). The antitumoral effect was only achieved *in vivo* following the use of *DOG1* knockdown. The effects seen *in vitro* with biochemical inhibition were attributed to off-target effects, also present in the *DOG1* knockdown cell lines. The second study is from our group, in which we used both *DOG1* inhibitor (T16_{inh}-A01) and activator (E-act), and observed modest effect on viability, proliferation, and apoptosis *in vitro*, even though we showed that inhibition, using T16_{inh}-A01, could act as a pro-apoptotic effector on early apoptotic GIST48 (an imatinib-resistant cell line) cells (28).

Several potent *DOG1* inhibitors now exist, and we have focused on one of the most potent ones possessing antitumoral properties, but also T16_{inh}-A01 that was used in our previous study (28). First, we show that chloride currents are inhibited following exposure to CaCC_{inh}-A01, in a dose-dependent and reversible manner. At 30 μ M the *DOG1*-current is inhibited by approximately 60%. In our experiments, we used the whole-cell configuration of the patch-clamp technique. In this setting, intracellular modulators, such as Ca²⁺, cAMP and inositol triphosphate (IP₃) are clamped and equilibrated with the pipette solution

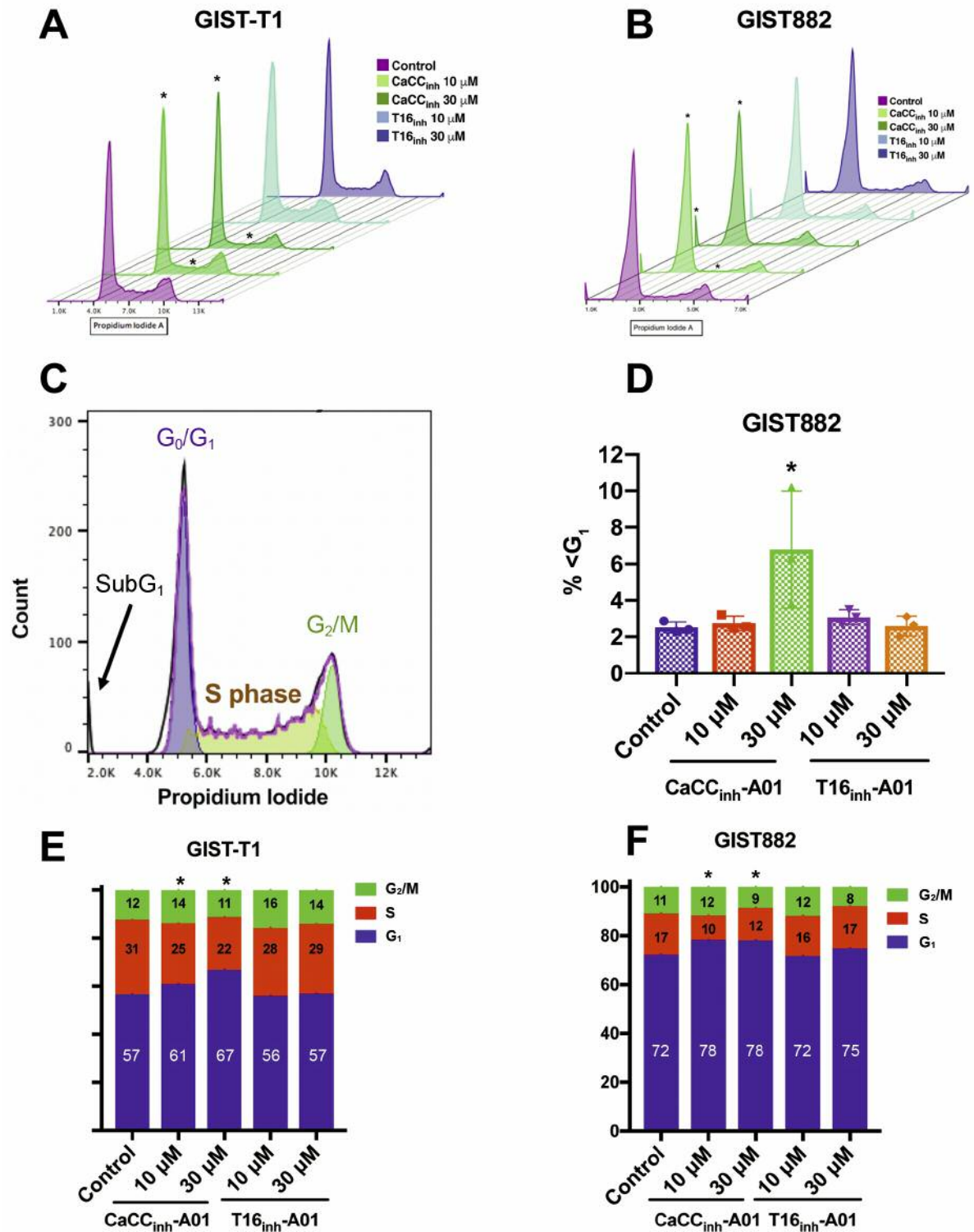


Figure 4. Flow cytometric analysis of the cell cycle. (A) and (B) show a representative histogram from cell cycle analysis, note in (B) definition of the different cell cycle phases. (C) Indicates the different distributions in the histogram. (D) Sub- G_1 analysis of GIST882 cells, shows significant increased amount of fragmented DNA in 30 μM CaCC_{inh}-A01 treated GIST882 cells. No sub- G_1 population was observed in GIST-T1 cell (shown in A). (E) and (F) Distribution of the cell-cycle phases in GIST-T1 and GIST882 cells, both demonstrating significant G_1 -cell cycle arrest following treatment with CaCC_{inh}-A01 at both 10 and 30 μM concentrations. Data represent mean \pm SD from three independent experiments. A-B and E-F analysis of variance was determined using two-way ANOVA with multiple comparison using Dunnett's test. For D Kruskal-Wallis test was used. * $p < 0.05$.

and omitting the potential impact of these modulators. Furthermore, the cells are voltage-clamped, and DOG1-current is evaluated at different membrane potentials. DOG1-current is dependent on intracellular Ca^{2+} -levels, and in low levels of $[\text{Ca}^{2+}]_i$ no chloride currents could be seen, well in accordance with our previous findings (28). Our conclusion from this set of experiments and previous finding are that $\text{CaCC}_{\text{inh}}\text{-A01}$ is a direct blocker of CaCC in GIST cells.

Secondly, cell viability is decreased in cells exposed to both inhibitors. GIST-T1 was more sensitive to $\text{T16}_{\text{inh}}\text{-A01}$ treatment compared to GIST882, with only 30 μM after 72 h affecting cell viability significantly. In general, $\text{CaCC}_{\text{inh}}\text{-A01}$ potently reduced cell viability in both cell lines, while $\text{T16}_{\text{inh}}\text{-A01}$ was more cell-specific, reducing viability more in GIST-T1 compared to GIST882. We used fully supplemented medium for viability assays in this study in contrast to another study using serum-starved cells with more potent effects on cell viability of DOG1 inhibition in prostate cancer with $\text{CaCC}_{\text{inh}}\text{-A01}$ and $\text{T16}_{\text{inh}}\text{-A01}$ inhibitors (23). Using serum-starvation (no FBS added to cell medium), 30 μM $\text{CaCC}_{\text{inh}}\text{-A01}$ had the best effect, and reduced cell viability by more than 50% over a 24-h time period in GIST-T1 cells (data not shown).

To assess the long-term effects of DOG1 inhibition, we used the colony formation assay during 10-14 days prior to readout. In GIST-T1 cells, $\text{CaCC}_{\text{inh}}\text{-A01}$ strongly reduced the ability to form colonies, from concentrations of 5 μM and above while $\text{T16}_{\text{inh}}\text{-A01}$ showed no significant effects on the colony forming ability of the cells. One possible explanation for this is that DOG1 is necessary for long-term cell survival. DOG1 knockdown in GIST *in vitro* did not lead to significantly reduced proliferation rates, even though such an effect has been demonstrated in a xenograft model *in vivo* (27). Secondly, degradation of DOG1 protein is ER-associated and does not occur immediately, but can take up to several days (29). Taken together, this might suggest that DOG1 degradation is necessary for long-term cell survival.

We also show that $\text{CaCC}_{\text{inh}}\text{-A01}$, but not $\text{T16}_{\text{inh}}\text{-A01}$, induces a cell cycle arrest in G_1 -phase. In addition to cell cycle arrest, we also observed in GIST882, but not GIST-T1, a sub- G_1 population of cells, indicative of apoptosis. The sub- G_1 population was significantly increased in $\text{CaCC}_{\text{inh}}\text{-A01}$ 30 μM treated cells. Only adherent cells were used in this study, which could possibly underestimate the proportion of apoptotic cells.

Even though off-target effects of DOG1 inhibitors cannot be excluded (33), a thorough study using a screening method to identify blockers of CaCC, and specifically DOG1, has identified that DOG1 protein degradation is necessary to achieve antitumoral effect (29). Noteworthy, DOG1-negative cells showed higher viability compared to DOG1-positive cells when exposed to DOG1 inhibitors. It was also shown that protein degradation was ER-associated and that the effect of degradation was observed after 24-48 hours. A

study on prostate cancer has shown that DOG1 inhibitors could induce apoptosis in prostate cancer cell lines through upregulating TNF- α signaling (23). TNF- α signaling occurred using both siRNA technology and biochemical inhibition using DOG1 inhibitors, suggesting similar mechanisms of action. Taken together, we interpret our findings that the antitumoral effects observed in this study are likely desirable on-target effects, with $\text{CaCC}_{\text{inh}}\text{-A01}$ being the most potent inhibitor in inducing antitumoral responses

The effect of the DOG1 inhibitors, not only on chloride currents, but also on DOG1 protein degradation, showed that this occurs after 24 h of treatment and increases over time (29). The colony formation assay examined the long-term effect on cell survival and showed a large difference between the two. It is likely that this effect is mediated by DOG1 protein degradation, since DOG1 is involved in proliferation, as it has also been shown in several knockdown models in epithelial cells as well as in GIST (14, 16, 27). Finally, we also report an effect on cell cycle that is in concordance with previous studies (29, 35). The G_1 -cell cycle arrest leads to slower proliferation of the cells. There was also a difference between the two inhibitors; $\text{CaCC}_{\text{inh}}\text{-A01}$ induced a statistically significant G_1 -cell cycle arrest, while $\text{T16}_{\text{inh}}\text{-A01}$ did not affect the distribution of the cells in the cell cycle. These data fit well with our data on viability and colony formation ability, and further support the notion that DOG1 is likely the mediator of long-term cell growth and survival.

In conclusion, we showed for the first time that DOG1 inhibition has antitumoral effects in the most common mesenchymal tumor of the gut, GIST. Inhibiting DOG1 affects the chloride current, causing G_1 cell-cycle arrest, while $\text{CaCC}_{\text{inh}}\text{-A01}$ strongly reduces cells ability to form colonies. This is likely mediated *via* DOG1 protein degradation. The outlined effects of DOG1 inhibition combined with its strong overexpression (>95%) among GIST patients makes it an attractive approach for the development of novel targeted biochemical GIST therapies.

Conflicts of Interest

None of the Authors declares a conflict of interest.

Authors' Contribution

RF, FS, and RB designed the experiments. RF, FS, CX, AZ and RB performed the experiments. RF, FS, CX, and RB performed the data analysis. RF and RB drafted the manuscript. All authors contributed to the interpretation of data, revised the manuscript and approved the final manuscript.

Acknowledgements

The study was financially supported by the Swedish Research Council, the Swedish Cancer Society, the Swedish Society of Medicine (Bengt Ihre grant), and the Cancer Society in Stockholm.

Financial support was also provided through the regional agreement on medical training and clinical research (ALF) between the Stockholm County Council and Karolinska Institutet.

References

- 1 Mastrangelo G, Coindre JM, Ducimetière F, Dei Tos AP, Fadda E, Blay JY, Buja A, Fedeli U, Cegolon L, Frasson A, Ranchère-Vince D, Montesco C, Ray-Coquard I and Rossi CR: Incidence of soft tissue sarcoma and beyond: a population-based prospective study in 3 European regions. *Cancer* 118(21): 5339-5348, 2012. PMID: 22517534. DOI: 10.1002/ncr.27555
- 2 Corless CL, Barnett CM and Heinrich MC: Gastrointestinal stromal tumours: origin and molecular oncology. *Nat Rev Cancer* 11(12): 865-878, 2011. PMID: 22089421. DOI: 10.1038/nrc3143
- 3 Blanke CD, Demetri GD, von Mehren M, Heinrich MC, Eisenberg B, Fletcher JA, Corless CL, Fletcher CD, Roberts PJ, Heinz D, Wehre E, Nikolova Z and Joensuu H: Long-term results from a randomized phase II trial of standard- versus higher-dose imatinib mesylate for patients with unresectable or metastatic gastrointestinal stromal tumors expressing KIT. *J Clin Oncol* 26(4): 620-625, 2008. PMID: 18235121. DOI: 10.1200/JCO.2007.13.4403
- 4 West RB, Corless CL, Chen X, Rubin BP, Subramanian S, Montgomery K, Zhu S, Ball CA, Nielsen TO, Patel R, Goldblum JR, Brown PO, Heinrich MC and van de Rijn M: The novel marker, DOG1, is expressed ubiquitously in gastrointestinal stromal tumors irrespective of KIT or PDGFRA mutation status. *Am J Pathol* 165(1): 107-113, 2004. PMID: 15215166. DOI: 10.1016/S0002-9440(10)63279-8
- 5 Schwab M: Amplification of oncogenes in human cancer cells. *Bioessays* 20(6): 473-479, 1998. PMID: 9699459. DOI: 10.1002/(SICI)1521-1878(199806)20:6<473::AID-BIES5>3.0.CO;2-N
- 6 Li J, Zhang H, Lu Y, Chen Z and Su K: Presence of PDGFRA and DOG1 mutations in gastrointestinal stromal tumors among Chinese population. *Int J Clin Exp Pathol* 8(5): 5721-5726, 2015. PMID: 26191287.
- 7 Huang F, Rock JR, Harfe BD, Cheng T, Huang X, Jan YN and Jan LY: Studies on expression and function of the TMEM16A calcium-activated chloride channel. *Proc Natl Acad Sci USA* 106(50): 21413-21418, 2009. PMID: 19965375. DOI: 10.1073/pnas.0911935106
- 8 Hartzell C, Putzier I and Arreola J: Calcium-activated chloride channels. *Annu Rev Physiol* 67: 719-758, 2005. PMID: 15709976. DOI: 10.1146/annurev.physiol.67.032003.154341
- 9 Paulino C, Kalienkova V, Lam AKM, Neldner Y and Dutzler R: Activation mechanism of the calcium-activated chloride channel TMEM16A revealed by cryo-EM. *Nature* 552(7685): 421-425, 2017. PMID: 29236691. DOI: 10.1038/nature24652
- 10 Choi EJ, Yun JA, Jabeen S, Jeon EK, Won HS, Ko YH and Kim SY: Prognostic significance of TMEM16A, PPF1A1, and FADD expression in invasive ductal carcinoma of the breast. *World J Surg Oncol* 12: 137, 2014. PMID: 24886289. DOI: 10.1186/1477-7819-12-137
- 11 Kulkarni S, Bill A, Godse NR, Khan NI, Kass JI, Steehler K, Kemp C, Davis K, Bertrand CA, Vyas AR, Holt DE, Grandis JR, Gaither LA and Duvvuri U: TMEM16A/ANO1 suppression improves response to antibody-mediated targeted therapy of EGFR and HER2/ERBB2. *Genes Chromosomes Cancer* 56(6): 460-471, 2017. PMID: 28177558. DOI: 10.1002/gcc.22450
- 12 Ubby I, Bussani E, Colonna A, Stacul G, Locatelli M, Scudieri P, Galletta La and Pagani F: TMEM16A alternative splicing coordination in breast cancer. *Mol Cancer* 12: 75, 2013. PMID: 23866066. DOI: 10.1186/1476-4598-12-75
- 13 Britschgi A, Bill A, Brinkhaus H, Rothwell C, Clay I, Duss S, Rebhan M, Raman P, Guy CT, Wetzel K, George E, Popa MO, Lilley S, Choudhury H, Gosling M, Wang L, Fitzgerald S, Borawski J, Baffoe J, Labow M, Gaither LA and Bentires-Alj M: Calcium-activated chloride channel ANO1 promotes breast cancer progression by activating EGFR and CAMK signaling. *Proc Natl Acad Sci USA* 110(11): E1026-1034, 2013. PMID: 23431153. DOI: 10.1073/pnas.1217072110
- 14 Jia L, Liu W, Guan L, Lu M and Wang K: Inhibition of calcium-activated chloride channel ANO1/TMEM16A suppresses tumor growth and invasion in human lung cancer. *PLoS One* 10(8): e0136584, 2015. PMID: 26305547. DOI: 10.1371/journal.pone.0136584
- 15 Mroz MS and Keely SJ: Epidermal growth factor chronically upregulates Ca(2+)-dependent Cl(-) conductance and TMEM16A expression in intestinal epithelial cells. *J Physiol* 590(Pt 8): 1907-1920, 2012. PMID: 22351639. DOI: 10.1113/jphysiol.2011.226126
- 16 Sui Y, Sun M, Wu F, Yang L, Di W, Zhang G, Zhong L, Ma Z, Zheng J, Fang X and Ma T: Inhibition of TMEM16A expression suppresses growth and invasion in human colorectal cancer cells. *PLoS One* 9(12): e115443, 2012. PMID: 25541940. DOI: 10.1371/journal.pone.0115443
- 17 Duvvuri U, Shiwardski DJ, Xiao D, Bertrand C, Huang X, Edinger RS, Rock JR, Harfe BD, Henson BJ, Kunzelmann K, Schreiber R, Seethala RS, Egloff AM, Chen X, Lui VW, Grandis JR and Gollin SM: TMEM16A induces MAPK and contributes directly to tumorigenesis and cancer progression. *Cancer Res* 72(13): 3270-3281, 2012. PMID: 22564524. DOI: 10.1158/0008-5472.CAN-12-0475-T
- 18 Ruiz C, Martins JR, Rudin F, Schneider S, Dietsche T, Fischer CA, Tornillo L, Terracciano LM, Schreiber R, Bubendorf L and Kunzelmann K: Enhanced expression of ANO1 in head and neck squamous cell carcinoma causes cell migration and correlates with poor prognosis. *PLoS One* 7(8): e43265, 2012. PMID: 22912841. DOI: 10.1371/journal.pone.0043265
- 19 Shiwardski DJ, Shao C, Bill A, Kim J, Xiao D, Bertrand CA, Seethala RS, Sano D, Myers JN, Ha P, Grandis J, Gaither LA, Puthenveedu MA and Duvvuri U: To "grow" or "go": TMEM16A expression as a switch between tumor growth and metastasis in SCCHN. *Clin Cancer Res* 20(17): 4673-4688, 2014. PMID: 24919570. DOI: 10.1158/1078-0432.CCR-14-0363
- 20 Liu F, Cao QH, Lu DJ, Luo B, Lu XF, Luo RC and Wang XG: TMEM16A overexpression contributes to tumor invasion and poor prognosis of human gastric cancer through TGF- β signaling. *Oncotarget* 6(13): 11585-11599, 2015. PMID: 25839162. DOI: 10.18632/oncotarget.3412
- 21 Liu J, Liu Y, Ren Y, Kang L and Zhang L: Transmembrane protein with unknown function 16A overexpression promotes glioma formation through the nuclear factor- κ B signaling pathway. *Mol Med Rep* 9(3): 1068-1074, 2014. PMID: 24401903. DOI: 10.3892/mmr.2014.1888
- 22 Liu W, Lu M, Liu B, Huang Y and Wang K: Inhibition of Ca(2+)-activated Cl(-) channel ANO1/TMEM16A expression suppresses tumor growth and invasiveness in human prostate carcinoma. *Cancer Lett* 326(1): 41-51, 2012. PMID: 22820160. DOI: 10.1016/j.canlet.2012.07.015

- 23 Song Y, Gao J, Guan L, Chen X and Wang K: Inhibition of ANO1/TMEM16A induces apoptosis in human prostate carcinoma cells by activating TNF- α signaling. *Cell Death Dis* 9(6): 703, 2018. PMID: 29899325. DOI: 10.1038/s41419-018-0735-2
- 24 Bill A, Gutierrez A, Kulkarni S, Kemp C, Bonenfant D, Voshol H, Duvvuri U and Gaither LA: ANO1/TMEM16A interacts with EGFR and correlates with sensitivity to EGFR-targeting therapy in head and neck cancer. *Oncotarget* 6(11): 9173-9188, 2015. PMID: 25823819. DOI: 10.18632/oncotarget.3277
- 25 Cao Q, Liu F, Ji K, Liu N, He Y, Zhang W and Wang L: MicroRNA-381 inhibits the metastasis of gastric cancer by targeting TMEM16A expression. *J Exp Clin Cancer Res* 36(1): 29, 2017. PMID: 28193228. DOI: 10.1186/s13046-017-0499-z
- 26 Li Q, Zhi X, Zhou J, Tao R, Zhang J, Chen P, Røe OD, Sun L and Ma L: Circulating tumor cells as a prognostic and predictive marker in gastrointestinal stromal tumors: a prospective study. *Oncotarget* 7(24): 36645-36654, 2016. PMID: 27153560. DOI: 10.18632/oncotarget.9128
- 27 Simon S, Grabellus F, Ferrera L, Galletta L, Schwindenhammer B, Mühlenberg T, Taeger G, Eilers G, Treckmann J, Breitenbuecher F, Schuler M, Taguchi T, Fletcher JA and Bauer S: DOG1 regulates growth and IGFBP5 in gastrointestinal stromal tumors. *Cancer Res* 73(12): 3661-3670, 2013. PMID: 23576565. DOI: 10.1158/0008-5472.CAN-12-3839
- 28 Berglund E, Akcakaya P, Berglund D, Karlsson F, Vukojević V, Lee L, Bogdanović D, Lui WO, Larsson C, Zedenius J, Fröbom R and Bränström R: Functional role of the Ca(2+)-activated Cl(-) channel DOG1/TMEM16A in gastrointestinal stromal tumor cells. *Exp Cell Res* 326(2): 315-325, 2014. PMID: 24825187. DOI: 10.1016/j.yexcr.2014.05.003
- 29 Bill A, Hall ML, Borawski J, Hodgson C, Jenkins J, Piechon P, *et al*: Small molecule-facilitated degradation of ANO1 protein: a new targeting approach for anticancer therapeutics. *J Biol Chem* 289(16): 11029-11041, 2014. PMID: 24599954. DOI: 10.1074/jbc.M114.549188
- 30 Ji Q, Guo S, Wang X, Pang C, Zhan Y, Chen Y and An H: Recent advances in TMEM16A: Structure, function, and disease. *J Cell Physiol* (6): 7856-7873, 2019. PMID: 30515811. DOI: 10.1002/jcp.27865
- 31 Berglund E, Berglund D, Akcakaya P, Ghaderi M, Daré E, Berggren PO, Köhler M, Aspinwall CA, Lui WO, Zedenius J, Larsson C and Bränström R: Evidence for Ca(2+)-regulated ATP release in gastrointestinal stromal tumors. *Exp Cell Res* 319(8): 1229-1238, 2013. PMID: 23499741. DOI: 10.1016/j.yexcr.2013.03.001
- 32 Hamill OP, Marty A, Neher E, Sakmann B and Sigworth FJ: Improved patch-clamp techniques for high-resolution current recording from cells and cell-free membrane patches. *Pflugers Arch* 391(2): 85-100, 1981. PMID: 6270629.
- 33 Wang H, Zou L, Ma K, Yu J, Wu H, Wei M and Xiao Q: Cell-specific mechanisms of TMEM16A Ca. *Mol Cancer* 16(1): 152, 2017. PMID: 28893247. DOI: 10.1186/s12943-017-0720-x
- 34 Boedtker DM, Kim S, Jensen AB, Matchkov VM and Andersson KE: New selective inhibitors of calcium-activated chloride channels - T16A(inh) -A01, CaCC(inh) -A01 and MONNA - what do they inhibit? *Br J Pharmacol* 172(16): 4158-4172, 2015. PMID: 26013995. DOI: 10.1111/bph.13201
- 35 Guan L, Song Y, Gao J and Wang K: Inhibition of calcium-activated chloride channel ANO1 suppresses proliferation and induces apoptosis of epithelium originated cancer cells. *Oncotarget* 7(48): 78619-78630, 2016. PMID: 27732935. DOI:10.18632/oncotarget.12524

Received April 10, 2019

Revised May 13, 2019

Accepted May 15, 2019